Wei-Lou Cao was born in Hunan, China, in 1942. He received the diploma from the China University of Science and Technology in 1966.

Since then he has been with the Shanghai Institute of Optics and Fine Mechanics, Chinese Academy of Sciences, Shanghai. Currently he is a Visiting Scholar at the University of Maryland, College Park. His research activities include the fusion laser system, nonlinear optics, picosecond phenomena, semiconductor lasers, and lunar laser ranging systems.

Jun-Da Ling was born in China. She received the B.S. degree in physics from Chaio Tung University, Shanghai, China.

From 1948–1953 she was an Instructor at the Physics Department at Hong Kong University, Hong Kong. From 1957–1964 she taught at the Peking Electronics Institute and the Institute of Science and Technology of the Chinese Academy of Sciences. Since 1965, she has been with the Shanghai Institute of Optics and Fine Mechanics of the Chinese Academy of Sciences, Shanghai, studying picosecond phenomenon. In the fall semester of 1980, she was a Visiting Scholar at the University of Maryland, College Park.

Chi H. Lee (M'79) received the B.S. degree in electrical engineering from the National Taiwan University, Taipei, Taiwan, and the M.S. and Ph.D. degrees in applied physics from Harvard University, Cambridge, MA, in 1959, 1962, and 1968, respectively.

He was with the IBM San Jose Research Laboratory from 1967 to 1968. Since 1968 he has been with the University of Maryland, College Park, where he is now a Professor of Electrical Engineering. His areas of research include picosecond phenomena, nonlinear optical effects, and millimeter-wave devices.

Dr. Lee is a member of Sigma Xi and the American Physical Society.

Application of a Two-Wavelength Picosecond Laser to Semiconductors

N. J. FRIGO, H. MAHR, AND DAVID J. ERSKINE

Abstract—**We report a two-wavelength (each of which is independently tunable) synchronously pumped picosecond laser which has large spectral separation, high conversion efficiency, and wide tuning ranges. The laser has been used to find the time-resolved reflectivity of a photoexcited semiconductor in the bandgap region. Unusually rapid relaxation of the screened excitonic reflectivity has been noted and a simple carrier diffusion model is proposed. The model also predicts results which agree with previously published data.**

I. Introduction

PICOSECOND studies of condensed matter have been a subject of intense interest in the last several years, and a major research tool in the picosecond experiments has been the synchronously pumped mode-locked laser [1], [2]. These lasers have several natural advantages. The very high repetition rates (10^8 Hz) allow sensitive detection techniques to be used, since high *average* powers do not require high *peak* powers. This permits their use in low quantum efficiency systems, while their pulse reproducibility over long experimental time allows signal averaging techniques to be exploited. The wide tuning ranges available make possible the examination of a variety of physical systems and, by tight focusing, the moderate intensities can be elevated to the GW/cm^2 range for high intensity experiments. Early experiments using such systems obtained their spectral and temporal resolution through a nonlinear upconversion light gate [3], [4] that analyzed the luminescence signal from a photoexcited sample. The advantage of such measurements is that they probe the occupation of real energy levels in the relaxing system, but they have the drawback that the efficiency and the resolution are inversely related. A technique that is complementary to the luminescence upconversion is the utilization of a second laser to probe the system after its photoexcitation by the first laser. The energy (spectral) resolution is the linewidth of the probe laser. If the probe is a synchronized picosecond laser, its pulse width is the time resolution, while if the probe is a CW laser, time resolution can be achieved by gating with the excitation pulse. Both types of lasers have been used, the first in a pump-probe technique [5], and the second in a "read-in, read-out" technique [6].

This paper describes a laser that is of the first variety, but it has several advantages that complement the earlier system. These inherent advantages accrue from the basic design of the cavity, and they allow a larger spectral separation between the pump and probe laser, much higher average powers, and very large tuning ranges. In the next section we describe the laser itself: its principles of operation, its cavity configuration, its performance, and its operating characteristics. In Section III

Manuscript received August 31, 1981. This work was supported in part by MSC/NSF Grant DMR-78-16751.

The authors are with the Department of Physics and Materials Center, Cornell University, Ithaca, NY 14853.

0018-9197/82/0200-0192$00.75

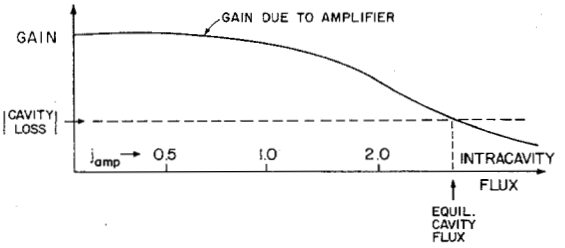

Fig. 1. Schematic representation of the nonsaturating roundtrip loss (dashed curve) and saturable gain (solid curve) experienced by a circulating ultrashort pulse, plotted as a function of normalized cavity flux j (see text). The laser will drive itself to the flux corresponding to the intersection of the two curves.

we describe the results of a preliminary experiment which illustrates the laser's utility in the study of photoexcited semiconductors and propose a simple model.

II. The Two-Wavelength Intersecting Cavity Laser

The standard synchronously pumped mode-locked laser uses a three-mirror cavity to focus the radiation tightly onto a free-flowing dye jet [7]. The cavity lengths of the dye laser and the mode-locked pumping laser are approximately equal so that gain is presented periodically to a circulating pulse whose cavity roundtrip time coincides with the pumping interval. This pulse arises from the cavity noise and adjusts itself in phase to meet the pumping pulse at the dye jet [4], [8]. One may estimate the circulating pulse flux by examining the overall gain associated with pulse propagation through saturable media [9]. Fig. 1 plots the energy gain experienced by a pulse in traversing a saturable gain medium (e.g., a pumped dye jet) as a function of the pulse's flux. A measure of the intracavity flux is $j = n\sigma/A$, where n is the number of photons in the pulse, σ is the stimulated emission cross section, and A is the beam's area at the medium. Thus j has an approximate physical description as the number of photons in the pulse that attempt to stimulate a transition. It can be shown [9], [16] that the ultrashort pulse, in traveling through a medium of optical thickness

$$Z_i = \int_0^l N(x)\,\sigma\,dx, \tag{1}$$

will have its flux amplified from j_i to j_f, where

$$\frac{e^{j_f} - 1}{e^{j_i} - 1} = e^{Z_i}. \tag{2}$$

Here, $N(x)$ is the population inversion density, σ is the stimulated emission cross section, and l is the thickness of the dye jet. Saturation effects become important when $j \approx 1$. For small signal levels the gain exceeds the loss. The flux then increases on each roundtrip until the circulating pulse reaches the steady-state flux for which the gain equals the loss, i.e., that j for which the gain and loss curves in Fig. 1 intersect.

The laser cavity may also include a saturable absorber. (A nonsaturable absorber presents an intensity *independent* loss which simply changes the magnitude of the "cavity loss" curve.) Appropriate choices of σ and A allow the absorbing

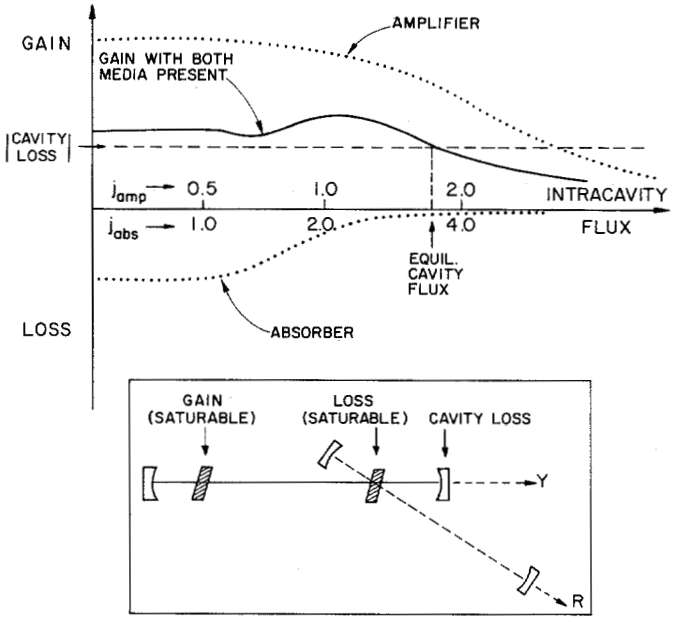

Fig. 2. Representation of gain and loss as in Fig. 1 but with saturable absorber also present (lower dotted line). Solid line represents total gain due to both saturable media. Inset: schematic of a two-wavelength intersecting cavity laser with two media in one cavity and one in the other.

jet to saturate before the amplifying jet, since a given intracavity flux yields a larger j for the absorber than the corresponding j for the amplifier. Naturally, the overall gain as a function of intracavity flux changes (see Fig. 2), but it is possible to saturate the absorber at relatively modest energy loss to the circulating pulse. If the saturable absorber is *itself* a laser dye, however, the addition of feedback (mirrors) to make a cavity completes *that* cavity's description as a synchronously pumped laser (see inset Fig. 2). Thus the second jet has two roles: in the first cavity (solid line) it contributes to the pulse forming process by being a saturable absorber [10], and in the second cavity (dashed line) it is a synchronously pumped gain medium. The two cavities intersect at a single spot in the second jet.

An interesting feature of the intersecting cavity laser is its unique combination of intracavity and extracavity characteristics. It has characteristics of *intracavity* pumping in the sense that the dye jet for the second cavity is inside the first cavity and its exposure to large cavity fluxes fully exploits the inherent nonlinearity of saturation. But since the two intersecting cavities are almost entirely distinct, the laser has the characteristics of *extracavity* pumping in the sense that the two lasers are nearly independent; the beams are distinct and can be tuned, filtered, and manipulated independently. This combination of characteristics occurs precisely because the two cavities overlap at only one point, obviating the need for dispersive separation.

The configuration which we use is shown in Fig. 3. The most obvious difference from the inset of Fig. 2 is that in both cavities the jets are surrounded by short focal length mirrors to increase j by decreasing the spot size. This laser has a number of convenient features. The output coupler of the first ("Y" or "yellow") laser can be flat or nearly flat so that the length

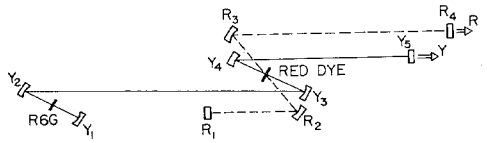

Fig. 3. Actual configuration of two-wavelength intersecting cavity laser. Solid line represents primary (yellow or "Y") cavity with amplifying and absorbing media present. Dashed line represents second (red or "R") cavity. Mirrors $R1$, $R4$, and $Y5$ are plane for convenience.

can be adjusted without the need to refocus at either jet. The "zig-zag" configuration reduces coma [11]. By using a four-mirror configuration for the second ("R" or "red") laser, again coma is reduced and the R_1-to-jet distance can be adjusted to equal the Y_5-to-jet distance, thus decreasing the "jitter" in the synchronization between the two pulses and decreasing the sensitivity of the red laser to cavity length mismatch. Qualitatively, the pulse forming process in both lasers is similar to that for the standard synchronously pumped laser [12], [4], [8]. In Fig. 2 the overall gain and loss is given for pulse passage through each jet. But relative to the overall gains, the "yellow" pulse sees more loss on its leading edge from the saturable absorber and more loss on its trailing edge from the gain medium. These two "compression" processes [9] are balanced by a temporal diffusion due to the frequency dispersion in the cavity [4], [12]. The "red" cavity is almost identical to the standard cavity but is pumped twice per period.

The laser that has been described here has several advantages over other types of two-wavelength picosecond pulse generation. Compared to intracavity two-wavelength methods, the intersecting cavity laser's most obvious advantage is that the wavelengths and cavity lengths of the two lasers can be tuned independently of each other. That is, since the beams are physically separate, each of the two beams can encounter distinct tuning elements and they can propagate in cavities with different physical lengths [14]. Another advantage of the intersecting cavity laser is the fact that since the two cavities are *optically* distinct as well, the mirrors do not have the same stringent requirements that would be necessary for a cavity that had mirrors exposed to both wavelengths.

Compared to parallel pumping configurations (for instance, an ion laser synchronously pumping two independent dye lasers), the present laser offers a more efficient use of the pump power, since only one threshold must be overcome, and hence higher average powers can be attained [15]. In addition, the spectral separations of the two outputs can be much greater for the intersecting cavity laser. For parallel pumping, both lasers experience a single Stokes shift away from the pump laser, while in our laser the second cavity suffers two Stokes shifts since it is pumped by the first. This extra Stokes shift has permitted us to achieve spectral separations as great as 1500 Å (0.45 eV) between the two output wavelengths.

Finally, we compare to a tandem pumping configuration in which the output of the first laser is used to pump the second laser, and sketch an interesting feature of intracavity pumped systems which we call "negative spectral feedback." If the yellow laser is being tuned to a spectral region for which the red dye absorption cross section is dropping, the red dye presents less loss to the yellow cavity. But if the loss in the yellow cavity decreases, then that cavity's flux (and hence the red laser pumping rate) increases. The red laser is then automatically pumped harder at exactly those spectral locations where it must be pumped harder. This negative spectral feedback greatly enhances the usefulness of the laser. In the tandem pumping configuration, the regions where the red laser's cross section is dropping require *more* yellow power to pump, steadily *decreasing* the power available for an experiment. Additionally, the intersecting cavity configuration allows operation in a higher j regime, which results in "flatter" output power characteristics due to more complete saturation [16] as Fig. 4 shows. Both of the "yellow" output curves yielded 8 ps pulses (we used a three-plate birefringent filter). Although for most of the tuning range the three-mirror configuration has a higher power output, the *usable* yellow power for the tandem pumping case is the total power minus the threshold for the second laser. Even assuming a constant red threshold of as low as 80 mW across the entire tuning range, one sees that the tuning range for the intersecting cavity laser is several times wider than that for the tandem pumped configuration.

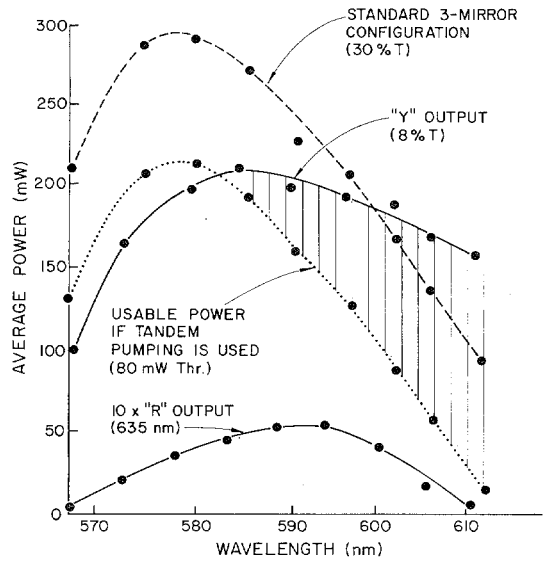

Fig. 4. Comparison of wavelength dependence of standard and intersecting cavity outputs. (Both yield 8 ps pulses in yellow.) Dashed curve is output from three-mirror configuration, upper solid curve is "yellow" output from two-wavelength configuration, lower solid curve is 10 times concomitant "red" output. Dotted curve is maximum usable output from three-mirror laser if as little as 80 mW is diverted to tandem pump a second laser. Note the much narrower tuning range.

The data in Fig. 4 were taken for an Ar^+ laser pumping rhodamine 6G and cresyl violet, but there is nothing that restricts one to these components. The technique should work for a variety of pump laser lines (e.g., 488, 647 nm in the ion laser series) and dye laser pairs (e.g., most rhodamines and oxazines). We have used a variety of dyes for the second jet; among them are nile blue, oxazine 720, oxazine 725, LD 690, and various mixtures to "tailor" the output. Fig. 5 shows a few of the possibilities to illustrate tradeoffs that are open to the user. The yellow autocorrelation widths were approximately 8 ps, the red autocorrelation widths were approximately 4 ps (we used a two-plate birefringent filter in the red cavity) and the cross correlations widths varied with power:

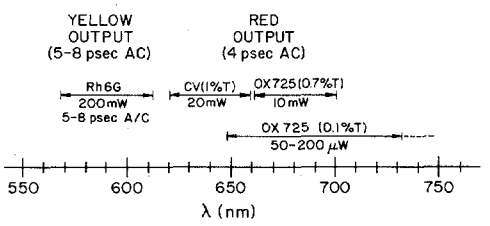

Fig. 5. Spectral characteristics of several different dye and coupling options.

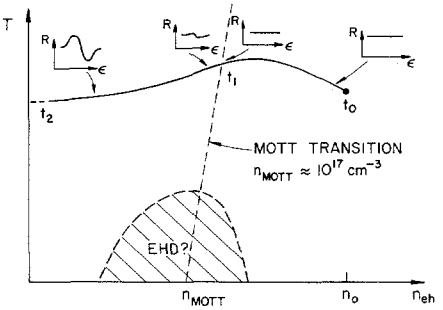

Fig. 6. Possible trajectory of photoexcited semiconductor in *e-h* density (n) and temperature (T) plane. At t_0, density n_0 is created and system relaxes through recombination, diffusion, internal conversion, etc. Phonon generation can change temperature as well. The reflectivity in excitonic region is featureless for densities greater than n_M but recovers as system relaxes below Mott density.

12 ps at 100 mW yellow power to 16 ps at 200 mW yellow power. For high power uses, cresyl violet and oxazine 725 span the range between 6200 Å and 7000 Å with 20 mW average power in CV and 10 mW in OX 725. These powers are high enough that they hold the possibility of attaining nonlinear optical effects using a combination of the two wavelengths. When a wide tuning range is desired, on the other hand, lower output coupling can trade power for tuning range. For instance, OX 725 was tuned over an 800 Å width, and the period of the tuning filter was reached before the dye gain dropped off. This degree of tuning range is unprecedented in such lasers.

In short, the intersecting cavity laser we are reporting here can be characterized as having large spectral separations between the two outputs, broad tuning ranges in both outputs, and flexibility in cavity, pump, and dye pair selection. Its high flux makes nonlinear processes accessible, and the high repetition rate allows a variety of sensitive detection techniques to be used.

III. Application: Reflectivity and the Diffusion of Carriers

In this section we present the results of a preliminary experiment in which we have applied our laser to study CdSe. (The experiment is an example of a use of the laser in which the flux from the shorter wavelength output drives a system into a nonlinear response and the second wavelength merely probes the system.) We are interested in following the fast processes which occur in direct gap semiconductors such as CdSe after intense photoexcitation. A rich variety of physical processes (Mott transition, electron-hole plasma, liquid, and droplets, etc.) have been hypothesized and experimental support for each has been reported [17]. Since in some cases the physical processes are expected to be mutually exclusive, the field is of inherent interest and not yet completely understood. Many optical experiments have been performed to ascertain which relaxation processes are taking place, and lasers with several nanosecond pulse durations have figured prominently [17]. Picosecond and subpicosecond transmission [18], luminescence [19], and gain [20] measurements have been performed on materials such as CdS, CdSe, and GaAs. Each of these types of experiments can be performed with our laser system, and each answers different types of questions about the relaxation processes occurring in the semiconductor. We report here an additional type of experiment, namely, what we believe is the first time resolved [21] reflectivity experiment performed in the bandgap region of a direct gap semiconductor under high photoexcitation [22]. The reflectivity measurement is of interest for several reasons: first, it is a "surface" probe (in the sense that only the properties within a wavelength of the surface are usually interrogated); and second, it is an ideal test for the existence of "oscillators," taken in the Lorentz sense to be two quantum levels. The oscillator we observe (located just below the band edge) is the Wannier exciton formed by the attraction of an electron in the conduction band and hole in the valence band. This type of measurement complements others, since it does not "integrate" the entire optical depth of the sample as do transmission experiments and does not have the ambiguity of determining the source of the photons as do luminescence experiments [23].

The experiment uses the two-wavelength laser first to excite the crystal with photons of energy above the bandgap, creating a high density of carriers in the conduction band, and then to probe the reflectivity of the relaxing crystal as a function of time and spectrum. There is not universal agreement on what should occur at low (LHe) temperatures after the photoexcitation, but it is clear that at high enough electron-hole (*e-h*) densities there should be a plasma state, and at very low *e-h* densities the system should condense into excitons. Between these two regions is a "Mott transition" [24] between the "conducting" plasma state and the "insulating" exciton state [25]. Mott's criterion for the transition is

$$n_M^{1/3} a_x \approx 0.2 \tag{3}$$

where a_x is the Bohr radius for an exciton in the solid, and n is the number density. For CdSe, this yields a Mott density of $n_M \approx 10^{17}$ cm^{-3}. After intense picosecond pulse excitation, a dense *e-h* plasma is created which screens out the formation of excitons; there are no excitons present, real or potential, since the oscillator (the two-level system) is no longer present in the excited region. As time proceeds, diffusion and recombination processes reduce the *e-h* density to values below n_M so that at later times the reflectivity of the excitonic oscillator will reappear. Fig. 6 sketches the process evolving from the initial system point as created by a short pulse at t_0 and possessing an initial temperature and density. As time progresses to t_1, the density decreases to the Mott density and then below. The temperature of the system can also vary as the system relaxes. We have not drawn in an intersection with an electron-hole liquid (EHL) coexistence curve since a calculation shows that

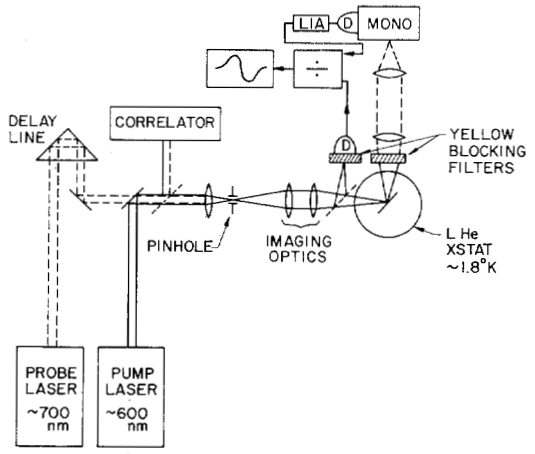

Fig. 7. Experimental setup. Pump and probe beams are spatially overlapped after temporal delay is set by delay line. Correlator provides real-time diagnostic auto- and cross correlations as experiment runs. Beams flood pinhole which is imaged to crystal surface, while red power is monitored to normalize reflectivity signal. Probe laser wavelength is scanned to provide excitonic reflectivity signature at each delay.

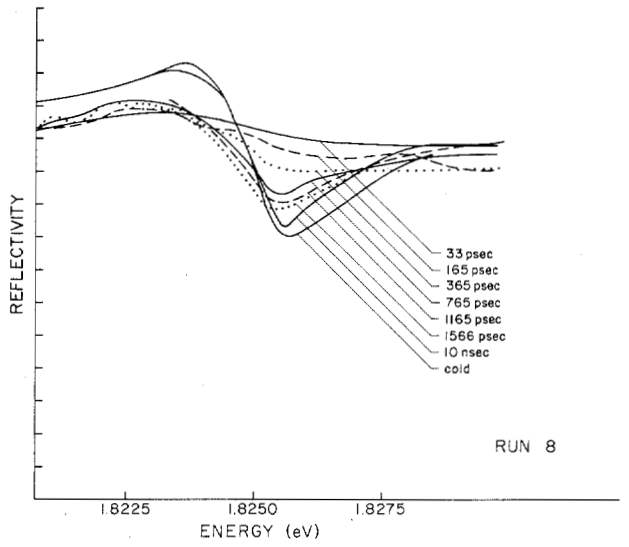

Fig. 8. Wavelength dependent reflectivity of CdSe at different times following photoexcitation. The exciton is screened at 33 ps but recovers quickly.

the steady-state lattice temperature in the excitation region is equal to or greater than the suggested EHL critical temperature [26].

The experimental apparatus we have used to examine this process is shown in Fig. 7. The pump and probe laser outputs are combined on a dichroic filter after a variable time delay is added to the probe laser pulse. To ensure that the pulses remain correctly spaced, we divert a small portion of the combined beams to a correlation setup so that auto- and cross correlations can be performed while the experiment is in progress. The combined beams "flood" a pinhole to reduce the spatial inhomogeneity of the Gaussian profiles and the pinhole is imaged onto the surface of the crystal immersed in superfluid helium. The light which is reflected from the crystal surface is monitored and is electronically divided by a portion of the light that goes through the pinhole. This divided signal is proportional to the crystal reflectivity. By scanning the probe laser wavelength through the excitonic region, we can observe the reflectivity for each time delay set by the delay line.

An example of reflectivity curves taken at a series of time delays shows (see Fig. 8) that the qualitative processes described (Fig. 6) are occurring. At the earliest time delay the exciton is completely screened out. Since $n_0 \approx 200\, n_M$ for this case (where n_o is the density of absorbed photons) and we have assumed a penetration depth of 0.1 μm [27], this is hardly surprising. What is quite interesting, however, is the unexpectedly rapid reappearance of the excitonic oscillator. Assuming a carrier diffusion of 1 μm in 1 ns [26] and a lifetime as short as 300 ps [19], [23], [28], one expects the density to exceed n_M for more than 1 ns, at which time the excitonic oscillator should begin to recover. The data show an almost *complete* recovery of the oscillator after 1 ns. We offer as a tentative explanation of this effect a carrier diffusion into the bulk of the crystal that occurs much more rapidly than has been assumed to date.

We assume that the carrier diffusion at these low temperatures is dominated by impurity scattering from the $n_i \approx 10^{16}$ cm^{-3} impurity density. By treating the impurities as ionized centers whose Coulomb potential is screened by the carrier plasma, an effective diffusion coefficient can be determined by using elementary kinetic theory and the Born approximation. We use the screened potential

$$V(r) = \frac{e^2}{\kappa r}\, e^{-\lambda r} \tag{4}$$

where κ is the static dielectric constant and λ is the Thomas–Fermi screening wavevector, given by

$$\lambda^2 = 4k_F/\pi a_x. \tag{5}$$

a_x is the excitonic Bohr radius, and k_F is the Fermi wavevector. For densities greater than n_M, this approach yields a density dependent diffusion coefficient of the approximate form (see Fig. 9)

$$D = D_0\, (n/n_M)^{\alpha}. \tag{6}$$

We have calculated $D_0 \approx 100$ and $\alpha \approx \frac{4}{3}$ taking ambipolar diffusion and full carrier screening into account [16]. At high densities the potential is more effectively screened so that the carriers diffuse rapidly away from the surface. As the density drops, however, the impurities become more efficient scatterers, and make the diffusion coefficient drop with density [29]. A numerical solution of the nonlinear diffusion equation shows that after only 10 ps, the carriers have diffused almost 2 μm into the crystal with a concomitant reduction by a factor of 20 in density. The solution also shows a very rapid reduction in density to below the Mott density. A drift velocity description (1 μm/ns) predicts a density that is everywhere *greater* than n_M after 1 ns, while the diffusion model predicts a density which is everywhere *less* than n_M after only 400 ps, at which point it is an order of magnitude lower than the drift velocity prediction. The reflectivity data in Fig. 8 do not rule out either a condensation to an EHL or a coexistence of excitons and plasma at densities below n_M, but do indicate

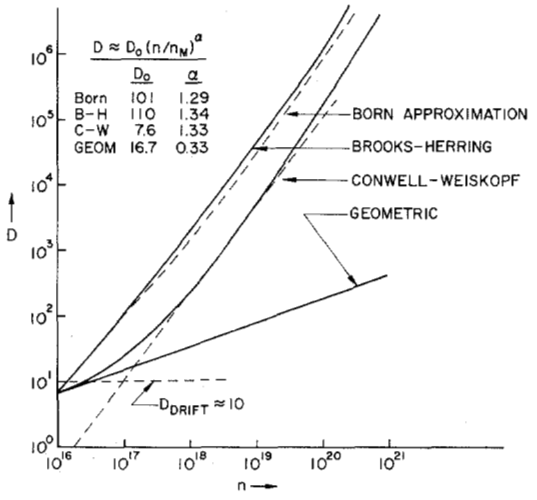

Fig. 9. Diffusion coefficients calculated for ambipolar carrier diffusion against plasma-screened impurity scattering in various approximations. "Geometric" refers to opaque scatterers.

that regardless of the ultimate fate of the *e-h* system, there may be early diffusion processes which must be taken into account.

The diffusion model can easily be extended to give approximate solutions for $n(t)$, the time dependent density of the EHP after ultrashort pulse (USP) excitation and n_{ss}, the steady-state plasma density achieved under nanosecond excitation. We find that

$$n(t) \approx n_0 \exp(-t/\tau) \times [1 + (1 + 2/\alpha)(n_0/n_M)^{\alpha} \cdot (D_0\tau/d_0^2)(1 - \exp(-\alpha t/\tau))]^{-1/(\alpha+2)} \quad (7)$$

for the time dependent density [30]. In this expression, τ is the carrier lifetime, and n_0 is the photon absorption density. Since n_0 is inversely proportional to d_0, $n(t)$ is independent of d_0 after very short times. The approximation to $n(t)$ agrees well with our numerical solution, since our fairly large excitation spot size (~40 μm) makes the diffusion essentially one dimensional. A feature of the diffusion model which gives us increased confidence is the fact that it can be used to interpret other data which have recently been published by Hoshida *et al.* Their luminescence measurements lead them to a calculated density as a function of time. Table I presents the data as read from Fig. 3(b) of their publication [32]. Using our own values of D_0 and α, and $\tau = 300$ ps, [23] we show in Table I densities calculated by (7). The agreement is quite good, especially since their n_0 was nearly twice ours and their excitation wavelength was 600 Å closer to the bandgap. In fact, the more general point that the peak density they observe is almost 15 times smaller than the density one would expect (i.e., n_0) supports the fast diffusion hypothesis. After ≈150 ps their data show a constant density of $\approx 3 \times 10^{17}$ cm^{-3}, a feature our model does not explain. However, the agreement at early times with their data and the rapid recovery of the excitonic reflectivity that we report lends credence to the possibility that very rapid carrier diffusion effects must be taken into account at early times to describe the relaxation of photoexcited semiconductors. The existence of such effects could influence such seemingly disparate areas as laser annealing, microstructure device design, and high-speed switching devices.

TABLE I
NORMALIZED DENSITIES AT EARLY TIMES AFTER PHOTOEXCITATION

TIME (psec)	EXP (Ref. 32)	CALC (Eqn. (7))
20	8	8.9
80	5	5.0
120	4	4.0
150	3	3.0

IV. SUMMARY

We have described a new two-wavelength picosecond laser which has the advantages of high output flux, independent tuning, broad tuning ranges, and large spectral separations. The laser augments devices which are currently being used to probe the relaxation of photoexcited semiconductors and has been used to obtain the first time resolved reflectivity spectrum near the bandgap of a photoexcited semiconductor. We have seen an unusually fast relaxation of the screening of the exciton and have proposed a carrier diffusion model that predicts the rapid recovery. The model also predicts results that, at early times, agree with previously reported experimental data.

ACKNOWLEDGMENT

N. J. Frigo would like to thank Prof. N. W. Ashcroft and Dr. J. Oliva for a series of very fruitful discussions.

REFERENCES

[1] C. V. Shank, E. P. Ippen, and S. L. Shapiro, Eds., *Picosecond Phenomena*, vol. 4, *Springer Series in Chemical Physics.* New York: Springer, 1978.
[2] R. Hochstrasser, W. Kaiser, and C. V. Shank, Eds., *Picosecond Phenomena II*, vol. 14, *Springer Series in Chemical Physics.* New York: Springer, 1980.
[3] H. Mahr and M. D. Hirsch, "An optical up-conversion light gate with picosecond resolution," *Opt. Commun.*, vol. 13, pp. 96–99, 1975.
[4] N. J. Frigo, T. Daly, and H. Mahr, "A study of a forced mode locked CW dye laser," *IEEE J. Quantum Electron.*, vol. QE-13, pp. 101–109, 1977.
[5] J. P. Heritage, "Vibrational dephasing measurements with CW mode-locked dye lasers," *Appl. Phys. Lett.*, vol. 34, pp. 470–472, 1979.
[6] E. P. Ippen and C. V. Shank, Eds., *Picosecond Phenomena*, vol. 4, *Springer Series in Chemical Physics.* New York: Springer, 1978, p. 103.
[7] H. Kogelnik *et al.*, "Astigmatically compensated cavities for CW dye laser," *IEEE J. Quantum Electron.*, vol. QE-8, pp. 373–379, 1972.
[8] C. P. Auschnitt, R. K. Jain, and J. P. Heritage, "Cavity length detuning characteristics of the synchronously mode-locked CW dye laser," *IEEE J. Quantum Electron.*, vol. QE-15, no. 9, pp. 912–917, 1979.
[9] G.H.C. New, "Mode locking of quasi-continuous lasers," *Opt. Commun.*, vol. 6, pp. 188–192, 1972; and "Pulse evolution in mode-locked quasi-continuous lasers," *IEEE J. Quantum Electron.*, vol. QE-10, pp. 115–124, 1974. These papers present a description of pulse propagation in saturable media under the rate equation approximation.
[10] Since most laser dyes can be viewed as ideal four-level media, the saturation of the second jet is desirable but not necessary for the laser to operate.
[11] M. H. Dunn and A. I. Ferguson, "Coma compensation in off-axis laser resonators," *Opt. Commun.*, vol. 20, pp. 214–219, 1977.

[12] H. A. Haus, "A theory of forced mode locking," *IEEE J. Quantum Electron.*, vol. QE-11, pp. 323–330, 1975.
[13] N. Frigo, C. Hemenway, and H. Mahr, "Cavity length stabilization technique for synchronously pumped mode-locked lasers," *Appl. Phys. Lett.*, vol. 37, pp. 981–984, 1981.
[14] Although the *physical* lengths of the two cavities are equal in intracavity pumped lasers, it is the *optical* lengths which must be made identical for synchronously pumped systems. See [4] and [8].
[15] This is equivalent to saying that slope efficiencies are greater than the overall efficiencies.
[16] This point will be amplified in a future communication.
[17] C. Klingshirn and H. Haug, "Optical properties of highly excited direct gap semiconductors," *Phys. Rep.*, vol. 70, pp. 315–398, 1981.
[18] C. V. Shank, R. L. Fork, R. F. Leheny, and J. Shah, "Dynamics of photoexcited GaAs band-edge absorption with subpicosecond resolution," *Phys. Rev. Lett.*, vol. 42, pp. 112–115, 1979.
[19] H. Yoshida, H. Saito, and S. Shionoya, "Time resolved spectra of spontaneous luminescence from high density electron-hole plasma in CdS," *Solid State Commun.*, vol. 33, pp. 161–165, 1980.
[20] K. Bohnert *et al.*, "Gain spectroscopy and plasma recombination in CdS," *Solid State Commun.*, vol. 27, pp. 295–299, 1978.
[21] By "time resolved" we mean that the experiment was not carried out in the steady-state (i.e., nanosecond) time regime.
[22] Shank *et al.* have measured reflectivity (C. V. Shank *et al.*, "Picosecond time resolved reflectivity of direct gap semiconductors," *Solid State Commun.*, vol. 26, pp. 567–570, 1978), but only at a fixed wavelength which was well above the bandgap.
[23] See T. Daly and H. Mahr, "Time resolved luminescence spectra from highly photoexcited CdSe at 1.8° K," *Solid State Commun.*, vol. 25, p. 323, 1978, and [19]. Of course, we "pay" for this advantage by not being able to determine the occupation numbers for the exciton.
[24] The "abruptness" of the Mott transition is still under investigation.
[25] N. F. Mott, *Metal-Insulator Transitions*. New York: Barnes and Noble, 1974.
[26] Using scaling laws (see T. L. Reinecke and S. C. Ying, "Scaling Relations for EHD condensation in semiconductors," *Phys. Rev. Lett.*, vol. 43, pp. 1054–1057, 1979), and T_c for CdS of 55 K (R. F. Leheny and J. Shah, "Condensation of optically excited carriers in CdS," *Phys. Rev. Lett.*, vol. 38, pp. 511–514, 1977), one arrives at $T_c \approx 28$ K for CdSe. This agrees with a theoretical prediction of 30 K given by M. Rosler and R. Zimmermann, "Phase diagram of EHL in polar semiconductors," *Phys. Status Solidi (b)*, vol. 83, pp. 85–91, 1977.
[27] R. B. Parsons, W. Wardzynski, and A. D. Yoffee, "The optical properties of single crystals of CdSe," *Proc. Roy. Soc. Ser. A.*, vol. 262, pp. 120–131, 1961.
[28] We assume that the luminescence lifetime is a lower bound for the carrier lifetime.
[29] One can view this as a transport equivalent of the Zener diode, with density corresponding to voltage and transport current corresponding to electrical current.
[30] The development of the expressions will be described more fully elsewhere.
[31] D_0 scales as n_i^{-1}.
[32] H. Yoshida, H. Saito, and S. Shionoya, "Picosecond relaxation processes of high density electron-hole plasma in CdSe," *Phys. Status Solidi (b)*, vol. 104, pp. 331–340, 1981.

N. J. Frigo, photograph and biography not available at the time of publication.

H. Mahr, photograph and biography not available at the time of publication.

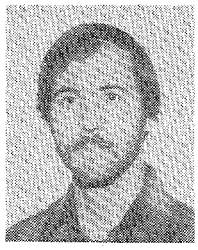

David J. Erskine was born in South Bend, IN, on May 19, 1957. He received the B.S. degree in physics from the University of Illinois, Urbana, in 1979.

He is currently a Research Assistant at the Dye Laser Facility, Cornell University Materials Research Center and is working toward his doctorate degree in solid-state physics.